International Journal of Chemical, Materials and Biomolecular Sciences
ISSN: 2415-6620
Vol:10, No:8, 2016

Study of Crashworthiness Behavior of Thin-Walled Tube under Axial Loading by Using Computational Mechanics

M. Kamal M. Shah, Noorhifiantylaily Ahmad, O. Irma Wani, J. Sahari

***Abstract*—**This paper presents the computationally mechanics analysis of energy absorption for cylindrical and square thin wall tubed structure by using ABAQUS/explicit. The crashworthiness behavior of AISI 1020 mild steel thin-walled tube under axial loading has been studied. The influence effects of different model's cross-section, as well as model length on the crashworthiness behavior of thin-walled tube, are investigated. The model was placed on loading platform under axial loading with impact velocity of 5 m/s to obtain the deformation results of each model under quasi-static loading. The results showed that model undergoes different deformation mode exhibits different energy absorption performance.

***Keywords*—**Axial loading, energy absorption performance, computational mechanics, crashworthiness behavior, deformation mode, thin-walled tubes.

I. INTRODUCTION

THE increasing number of deaths in road accidents associated with growth number of vehicles around the world shows the importance to study the crashworthiness behavior. Thin-walled tubes are designed to convert the kinetic energy to plastic-strain energy as an energy absorption device to absorb impact energy during collision and protect the passenger in the vehicle. As a typical class of energy absorbers, thin-walled structures have been widely used in crashworthiness applications such as automotive industry to protect passengers from severe injury because of their excellent energy absorption capacity and lightweight. According to [1], thin-walled tube structures with different shapes of the cross-sections are widely used in various transportation systems as energy absorbing components to dissipate the kinetic energy during violent collisions and crashes. Fig. 1 is an example of the application thin walled tube in front of trains and in longitudinal frames of automobiles [1].

Alavi Nia et al. [2] studied the effects of buckling initiators on mechanical behavior of thin-walled square tubes subjected to oblique loading. Their findings show that initiators changed the deformation mode of specimens from global buckling mode to progressive buckling and reduce a considerably amount of peak load. Their studies showed the relationship between loading angles on specimens with crushing force efficiency. Badnava et al. [3] had conducted an experimental investigation on crack effect on the mechanical behavior and energy absorption of thin-walled tubes. The findings show that crack effects can reduced about 4.92% to 31.33% of peak load for cylindrical thin-walled tubes and 2.55% to 18.52% of peak load for square thin-walled tubes. The presence of crack also increases the crush force efficiency by 67% and 31% for cylindrical and square thin-walled tubes respectively. Lu et al. [4] conducted a research on quasi-static axial compression of thin-walled tubes with four types of geometries experimentally. Their experimental results show that increase in number of inward corners shows an improvement in energy absorption efficiency but until certain extent. Their findings show that further increasing in numbers of inwards corner to 16-sided star; the energy absorption performance however, has decreased.

In this paper, axial loadings are placed on square and circular thin-walled tube geometry model under an impact velocity of 5 m/s. The graph of load against crushing displacement for each specimen are obtained through computational values and compared. The deformation mode of each model subjected to axial loading are studied and explained. Then, the energy absorption properties of each specimen are calculated and compared and the best energy absorption device among the specimens is proposed.

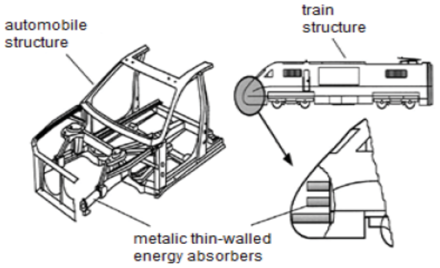

Fig. 1 Thin Walled Tubed as Energy Absorber Elements for Trains and Automobiles

---

M. Kamal M. Shah is with the Deputy Director Material and Mineral Research Unit, University Malaysia Sabah, Kota Kinabalu, Malaysia, (e-mail: mkamalms@ums.edu.my)

Noorhifiantylaily Ahmad and J. Sahari are with University Malaysia Sabah (e-mail: noorhifiantylaily@yahoo.com, sahari@ums.edu.my).

Irma Wani O. is with the Centre for the Promotion of Knowledge and Language Learning Department, University Malaysia Sabah, Kota Kinabalu, Malaysia, (e-mail: iwoppibs@gmail.com.my).

According to Isaac and Oluwole, modeling parameters are the parameters which are used in this work for comparison use as well as readings that are obtained from the load displacement curve. The parameters equations are stated below with their explanations [5]. Maximum crushing load, P_{max} is the maximum compressive force experienced by the specimens during axial compression process. It often occurs at the initial stage of the loading when the first buckling forms. This parameter indicates the maximum load that can be sustained by the specimens before plastic deformation takes place. Mean crushing force Pm is given by:

$$P_m = \frac{1}{d} \int_0^{\delta} P(\delta)\, d\delta \qquad (1)$$

where $P(\delta)$ is the instantaneous crushing load which corresponds to the instantaneous shortening δ. By Integrating the area under the load displacement curve, (1) gives the energy absorption E which is expressed as:

$$E_a = \int_0^{\delta} P(\delta)\ d\delta \qquad (2)$$

Crush force efficiency, CFE, is used to compare the efficiencies of energy absorbers and is defined as the ratio of mean crushing force over maximum crushing loads:

$$CFE = \frac{P_m}{P_{max}} \qquad (3)$$

Specific energy absorption, SEA, is amount of energy absorbed per unit mass, M. Measure the capability of different energy absorbed materials. By decreasing the absorber mass, high values of SEA can be obtained:

$$SEA = \frac{E_a}{M} \qquad (4)$$

II. METHODOLOGY

The methodology was broken up into three phases which is Pre-Processing, FEA stages and Post-Processing. The computational mechanics of crashworthiness test were conducted using a commercial finite element analysis software ABAQUS 6.14, analysis code ABAQUS/explicit product. The reference model geometry used for the analysis are comparing with three different type of length 120 mm, 100 mm and 80 mm. Each of model geometry has two types of cross sectional geometry which is cylinder and square with constant thickness 1 mm. Table I shows the model dimension of thin walled tube.

Table II is the chemical properties and Table III is the mechanical properties of AISI 1020 used for each model for this analysis. The element model is assigned with a specific mechanical property of AISI 1020 steel.

The plastic initiation criteria were set up in Johnson Cook plasticity model. The material constants of the Johnson Cook model for AISI 1020 steel are listed in Table IV [6].

Fig. 2 shows the upper and lower of reference point the body part. The impactor (Upper Plate) and base (Lower Plate) were both encapsulated by the body part model. Lower plate was set as tie contact to the body model as a boundary condition for the test. General contact was set at upper plate as the impactor, the axial load which is not fixed to the circumference of the body model and was assigned the tangential behavior where the coefficient of friction for metal structure is 0.2.

TABLE I
MODEL DIMENSIONS OF THIN WALLED TUBE

Code	Shape	Side/diameter (mm)	Length (mm)
C120	Circular	48	120
C100		48	100
C80		48	80
S120	Square	50	120
S100		50	100
S80		50	80

TABLE II
CHEMICAL COMPOSITION OF AISI 1020 STEEL

Element	Content (%)
Iron, Fe	98.778
Carbon, C	0.18
Silicon, Si	0.18
Manganese, Mn	0.79
Phosphorous, P	0.014
Sulphur, S	0.049
Aluminium, Al	0.002
Nitrogen, N	0.007

TABLE III
MECHANICAL PROPERTIES OF AISI 1020 STEEL

Properties	AISI 1020 steel
Young's Modulus (GPa)	200
Poisson's ratio	0.29
Yield stress (MPa)	265

TABLE IV
MATERIAL CONSTANTS OF JOHNSON-COOK MODEL FOR AISI 1020 STEEL

Parameter	Descriptions	Value
A (MPa)	Material Parameter	187.6
B (MPa)	Material Parameter	199.1
N	Strain Power Coefficient	0.1717
C	Material Parameter	0.06324
M	Temperature Power Coefficient	0.4437
ε^0 (s^{-1})	Reference Strain Rate	1
ρ (kg/m^3)	Density	7870
$C_{p\ (J/kg.K)}$	Specific Heat	448

The boundary conditions were chosen to simulate the impact of a heavy mass over the top surface of the tubes that remained in contact throughout the transient phase of deformation. The models were meshed using shell elements as shown in Fig. 3. This was done to reduce the computational time required as well as for better predictions as compared to usual solid elements in the case of thin walled structures.

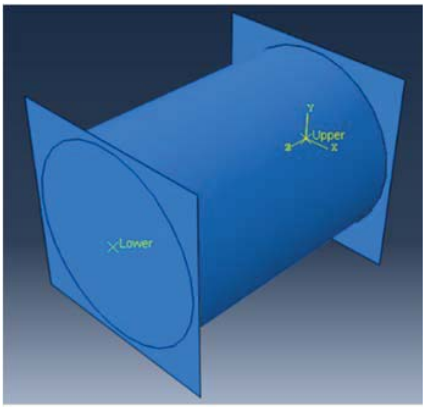

Fig. 2 Assembly of Part Model

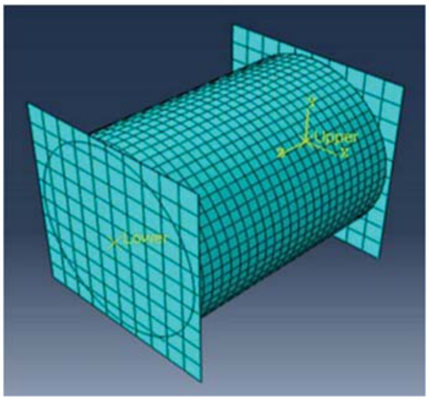

Fig. 3 Meshing of Element

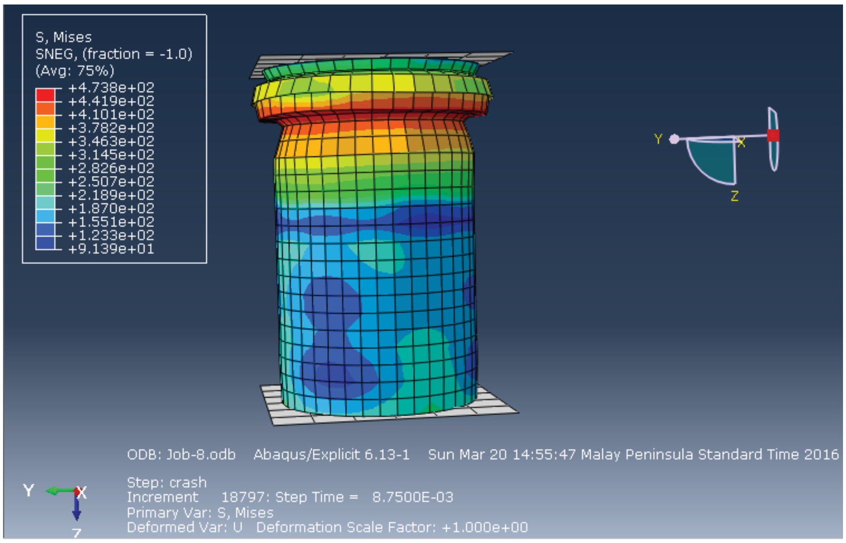

ODB: Job-8.odb Abaqus/Explicit 6.13-1 Sun Mar 20 14:55:47 Malay Peninsula Standard Time 2016

Step: crash
Increment 18797: Step Time = 8.7500E-03
Primary Var: S, Mises
Deformed Var: U Deformation Scale Factor: +1.000e+00

Fig. 4 Deformation of Cylindrical Tubed under Axial Loading

After the design has been completed, the simulation is run for cylindrical and square tube. The analysis is repeated with three different lengths for each geometry under axial loading, as shown in Fig. 4 is the deformation of cylindrical tube, the results of maximum loading of each test is taken directly from program.

III. RESULTS

The crushing mode deformation AISI 1020 mild steel for square undergoes non-symmetric crushing mode deformation or known as diamond pattern. As illustrated from Table V, cylindrical thin walled tube indicates dissimilar crushing mode when 120 mm and 80 mm model length used, which is exhibit concertina crushing mode pattern. Length of model influenced the crushing deformation and SEA performance of thin walled tube. The higher the model length used, the great number of folds created in thin walled tubed model.

The results of square and circular thin-walled tube stated and explained under different sections are shown in Figs. 5-7. The graph load against crushing displacement for each model is plotted to determine peak force and energy absorption of thin walled tube model, comparing the crushing load displacement curve can help analyze behaviors of different geometry model. The total energy absorption value is calculated from area under the graph of crushing load against displacement.

TABLE V
CRUSHING MODE DEFORMATION RESULT

Shape	**Length (mm)**		
	120	100	80
Cylinder	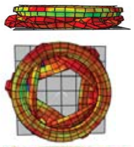	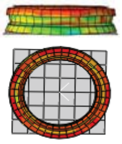	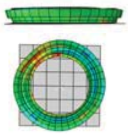
Square	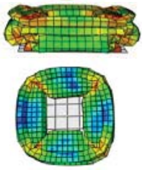	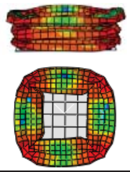	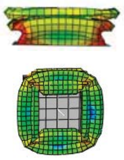

The purpose of an energy absorber is to continue low crush forces conversely reaching high energy levels. When the crush force is high, the force transmit to the passengers and vehicle components will be high.

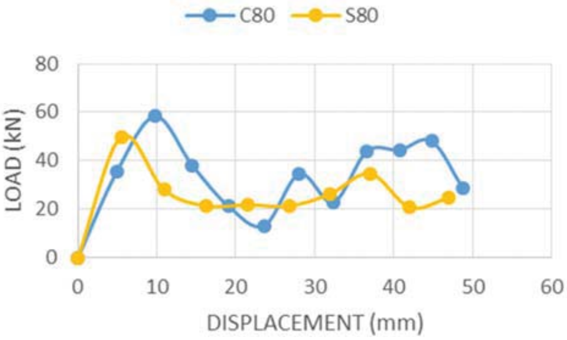

Fig. 5 Load-displacement curves for model length 80 mm

From Fig. 5, there is total four peak axial loading values throughout the axial loading test for cylinder and three peak load for square. The general load displacement characteristics of all tube can be defined by a rapid rise of the peak load. The load was observed when one end of the tube models started folding. The upper and lower graph curve for thin walled tube of the load values started from large then damped gradually with compression progress until reaching stable load. It is noted from the simulation that the deformation mode of model when subjected to axial loading is progressive buckling. But, for the square, the first lobe does not occur on the top part of model, but rather the lower part of the model. The distance between the lobes of model was found to be bigger than S100 and S120. The total energy absorbed for cylinder and square by the model during plastic deformation is found to be 1437.7732 J and 1238.0348 J for model length 80 mm.

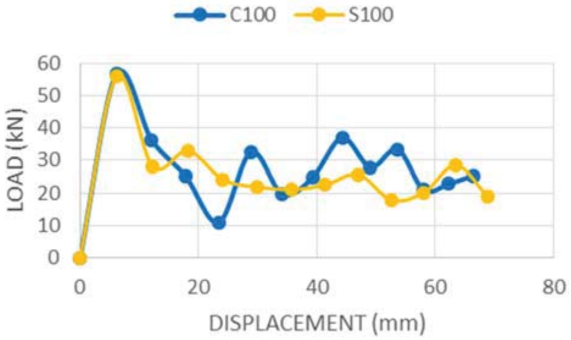

Fig. 6 Load-displacement curves for model length 100 mm

From Fig. 6, there are total four peak load for both model geometry length 100 mm. Peak load cause total distortion and a permanent change. The highest crushing load the most important biomechanical factor which must be kept below the allowable value when designing an energy absorbing material. The higher number of total peak load, the great number of folds created in thin walled tubed model. It is observed that the deformation model of S100 is the same as S80 which is progressive buckling that exhibits diamond shape folding when experienced plastic deformation. The deformation mode of C100 and C80 is similar which deformed in axisymmetric deformation mode when subjected to axial loading. The folding is in concertina shape. While for S100 is diamond shape which is progressive buckling that is similar to previous model S80. The total amount of energy is found through integration of area under the curve of Fig. 6 by the model during plastic deformation is found to be 1858.6686 J and 1780.3103 J for cylinder and square model length 100 mm.

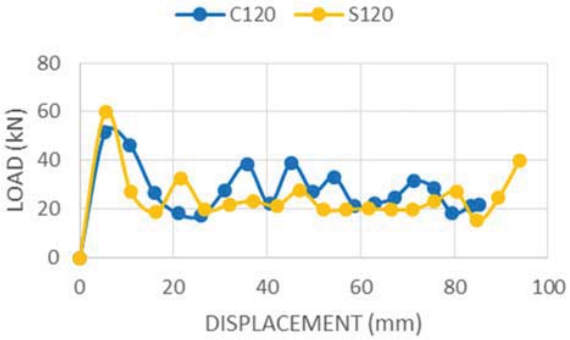

Fig. 7 Load-displacement curves for model length 120 mm

From Fig. 7, both mild steel geometry of thin walled tubed show a slightly upward trend at the end crushing distance. The load carrying capacity continues to increase for model geometry length 120 mm compare to previous length 100 mm and 80 mm, this graph trend solution can be characterized as buckling bifurcation point, stable. Which is the loading is completely removed from the model when the upper plate is lift off from it. Both model deformed totally without leaving any intact part. The reason is due to diamond deformation mode tends to create a larger gape between each lobe compare with axisymmetric deformation mode. The collapse load for model length 120 mm higher than previous model length 80 mm and 100 mm. The total peak crushing force is increased with increasing the model length of mild steel thin walled tubed. The total energy absorption of cylinder is 2405.5852 J and square is 2155.8416 J for model length 120 mm.

Table VI is the parameter result of crashworthiness thin walled tube for this model analysis when impact load is applied.

From Fig. 8, a significant increase of energy absorption (EA) is seen to increase gradually with model length. The longest model length 120 mm have greater energy absorption compare to the shortest model length 100 mm and follow by 80 mm. Reduced tube length provides lower EA and increased tube length produce considerable higher EA. The total energy absorption of cylinder is higher than square thin walled tubed. Thus, circular thin-walled tubes are capable of absorbing more energy when the length of model longer.

Fig. 9 shows the bar chart of crushing force efficiency thin walled tubed model when axial load is applied. The crushing force efficiency is the expression of the impact response of the structure. This is important in measuring the uniformity of crushing load. The percentage of CFE calculated from the ratio of mean crushing force to the peak force. The CFE indicates the effectiveness of vehicle structure, in case of a crush and the value of CFE will increase with the proportionally diminishing value of the peak load. The high CFE value model S80 indicates a low peak load withstand on thin walled tube model and leads to decreased passenger safety when impact load is applied. This chart shows that the lower the CFE the better the performance of the energy absorption structure. The crushed length of column thin walled tubed cylinder and square decreased with increase side length. Thus, the increase in column side length increased its resistance to buckle, the plastic energy stored due to the permanent deformation of the columns also increased.

From Fig. 10, it is shown that for circular thin-walled tube, the specific absorbed energy increases as the model length increases. The chart shows, the longest model length 120 mm have greater SEA compare to the shortest model length 100 mm and follow by 80 mm. Overall, SEA is a measured of the capability for different energy absorbed materials. By decreasing the absorber mass, high values of SEA can be obtained. It is clearly shown that, in case of an increased length 80 mm, 100 mm to 120 mm SEA capacity of the model were raised.

It is found that among the two cross-sections model, the better energy absorption device is selected to be circular thin-walled tubes. The best energy absorption device is selected to be model CODE = C120, which is circular thin-walled tube of 120 mm model length. Firstly, the energy absorption of C120 is 2405.5852 J among the highest from all the model. It is favorable to choose the model with highest energy absorbing device, as it is easier to deform thus absorb much of the impact energy away when the collision is made. Secondly, which indicates the crush force efficiency of C120 is expected to be the lowest among the three-model length cylinder. Lastly, it is important that tubes of high values of SEA be chosen in order to maximize the energy absorption while keeping the light weight properties of the specimen. The amount of SEA value of C120 is once again the highest among all the model, which is 17256.7088 J/kg. The high SEA value shows that the model is capable of absorbed higher amount of energy when it experienced impact.

TABLE VI
PARAMETERS RESULT FOR THIN WALLED TUBE MODEL

Model	E_a (J)	P_{max} (kN)	CFE (%)	SEA (J)
C80	1437.7732	58.2751	50.62	15476.5684
C100	1858.6686	56.5863	49.49	15995.4269
C120	2405.5852	51.5986	48.97	17256.7088
S80	1238.0348	49.9259	52.73	10032.6969
S100	1780.3103	55.8513	46.32	11537.9800
S120	2155.8416	60.0326	43.57	11646.9022

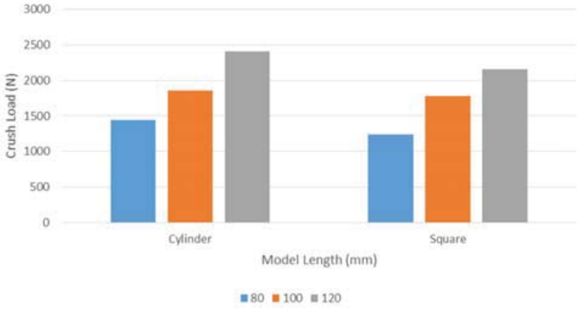

Fig. 8 Energy Absorption

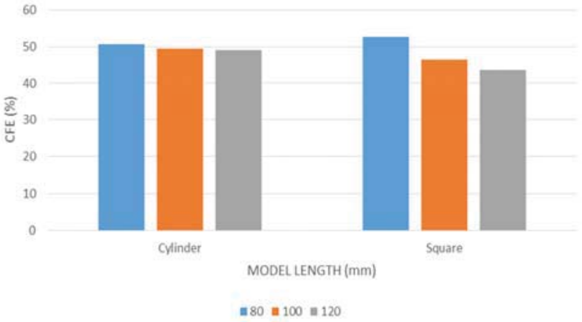

Fig. 9 Crushing Force Efficiency

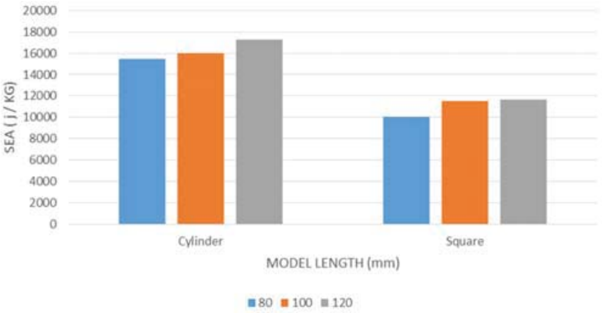

Fig. 10 SEA

IV. CONCLUSION

This paper presented the study of crashworthiness behavior of mild steel thin-walled tube by analyzing its energy absorption performance of each model using computer mechanics, ABAQUS software. Axial loading test had been carried out to determine the crushing behavior of thin-walled tube model under axial loading. Load-displacement curves are plotted based on result values. The deformation mode of model is then explained from load-displacement curve, and the model geometry parameters which determine the energy absorption characteristics of model were calculated and tabulated in Table I. Graph of EA, CFE and SEA were plotted against model respectively, the graphs were explained. The crashworthiness behavior of thin walled tube using computational mechanics successfully conducted. This study can be concluded as:

- The crushing mode behavior of all model undergoes diamond crushing mode pattern except for cylinder model length 120 mm experience concertina crushing mode.
- The cross-sectional geometry affects the crashworthiness behavior of thin walled tubed. Cylinder have the best energy absorption compare to square.
- The length had influence on the energy absorption of thin walled tubed. Highest length of thin walled tube has greatest energy absorption compare to lowest length.
- The best energy absorption among all model selected to be model C120. C120 is capable to deform very quickly under impact loading and absorbed the highest amount of impact energy when it undergoes plastic deformation.

ACKNOWLEDGMENT

We would like to take this opportunity to express our deepest appreciation and gratitude to those people who had guided and assisted us doing this research. We thank our colleagues from University Malaysia Sabah who provided insight and expertise that greatly assisted the research, although any errors are our own and should not tarnish the reputations of these esteemed persons.

REFERENCES

[1] Marsolek, J. a.-G. (2004). Energy absorption of metallic cylindrical shells with induced nonaxisymmetric. International Journal of Impact Engineering, vol. 30, 1209-1223

[2] Alavi, N., A.A., Nejad, K. F., Badnava, H., & Farhoudi, H. (2012). Effects of buckling initiators on mechanical behaviour of thin-walled square tubes subjected to oblique loading. Thin Walled Structures, 59: 87-96.

[3] Badnava, H., Nia, A. A., & Nejad, K. F. (2001). An experimental investigation on crack effect on the mechanical behaviour and energy absorption of thin-walled tubes. Materials and Design, 32: 3594-3607.

[4] Lu, G., Fan, Z., & & Liu, K. (2013). Quasi-static axial compression of thin-walled tubes with different cross-sectional shapes. Engineering Structures, 55, 80-89.

[5] Isaac, C., & Oluwole, O. (2015). Finite Element Comparative Analysis of the Crushing Behaviour of Square Steel Tubes. International Journal of Scientific & Engineering Research, 6: 1650-1655.

[6] Huang, C.-C. (2013). A Study on Tube Neck-spinning Process at Elevated Temperatures. Hsinchu, Taiwan.